Geothermal Exploration at Mount Meager, Southwestern BC: A Regional Resistivity Model from 3-D Inversion of Broadband Magnetotelluric Data

Cedar Hanneson and Martyn J. Unsworth
University of Alberta, Department of Physics

Summary

The Garibaldi volcanic belt in northwestern North America is part of the ring of fire, a belt of volcanic activity that surrounds the Pacific Ocean. Many countries in this region produce electricity from hot water extracted from geothermal reservoirs found beneath these volcanoes, and Canada could do the same. The most recent volcanic activity in the Canadian Garibaldi belt occurred around 350 BC at Mount Meager. Steam vents on this volcano have become active in recent years and major landslides have occurred, including an event in 2010 that remains Canada's largest recorded landslide.

Geothermal research has taken place at Mount Meager since the 1970s and suggests that a 200 MW power plant could be economic. To reduce the economic risks of development, additional information about the geothermal reservoir and natural hazards is needed. This can be obtained from geophysical studies of the subsurface.

In 2019 and 2020, broadband magnetotelluric data were collected in the region around Mount Meager. They were used to generate a 3-D model of electrical resistivity, a property that is sensitive to the presence of fluids. This model gives valuable information about fluid flow and potential geothermal reservoirs, as well as the size and location of a magma body beneath this active volcano.

Introduction

Offshore southwestern British Columbia and northwestern Washington, the Juan de Fuca plate subducts beneath the North American plate at the Cascadia subduction zone (Fig. 1). This subduction zone is a young, warm endmember; therefore, the subducting plate in the fore arc is 300-600^{o}C hotter than an old, cool endmember such as the Pacific plate in northeastern Japan (Savard et al. 2018). The Juan de Fuca plate is 0-11 million years old at the Cascadia subduction zone, in contrast to the 120–145-million-year-old Pacific plate at the Tohoku subduction zone (Jones 2019).

Dehydration reactions in the subducting slab release volatiles into the overlying mantle of the North American plate, lowering its melting point and creating a region of partial melt, which leads to volcanism at the surface above (Stern, 2002). The resulting chain of volcanoes is called the Cascade volcanic arc. The northern segment, from Glacier Peak to Silverthrone, is called the Garibaldi volcanic belt (GVB); and the southern segment, from Mount Rainier in central Washington to Mount Lassen in northern California, is called the High Cascades (Mullen et al., 2017).

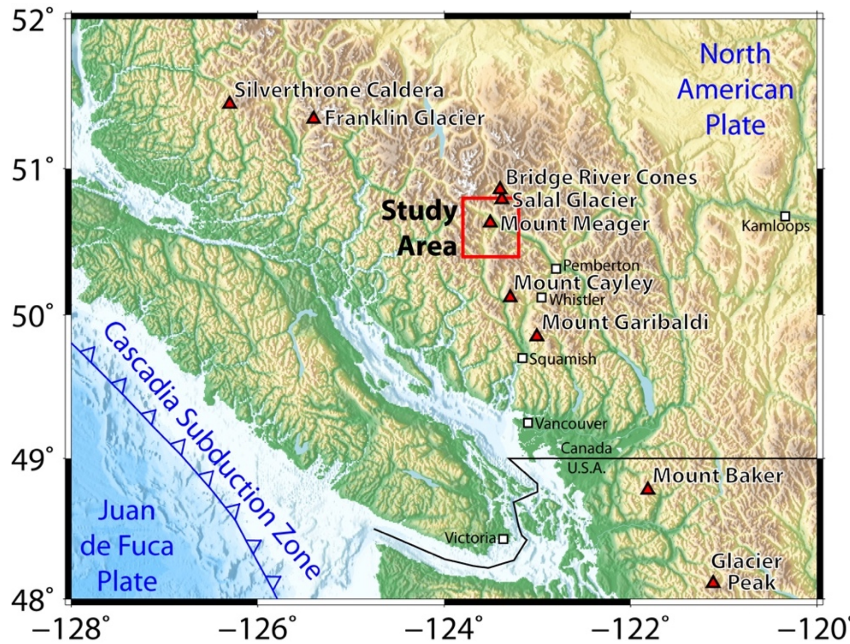

Figure 1*: Map of southwestern BC and northwestern Washington. Holocene volcanic centers in the Garibaldi volcanic belt are shown as triangles and population centres are shown as squares.*

The GVB trends NW-SE and is 300-400 km inboard of the trench, whereas the High Cascades trend N-S and are 250-300 km inboard (Hickson, 1994). Mount Baker is the most voluminous volcanic complex in the GVB, Glacier Peak is the most-recently active with an eruption in the mid-1700s, and Mount Meager is the most-recently active in Canada with a major eruption ~2400 years ago (Hickson, 1994). Recent volcanism in the GVB has been rhyolitic-to-dacitic at Mount Meager, dacitic at Mounts Cayley and Garibaldi, and andesitic at Mount Baker and Glacier Peak (Hickson, 1994). This illustrates a change from felsic composition in the north to intermediate silica content in the south.

The Mount Meager area drew attention as a geothermal target because of two thermal spring systems, Meager Creek springs and Pebble Creek spring (Souther, 1981). Early work included geothermometry, DC resistivity, and diamond drilling (Fairbank et al., 1981). Lewis and Jessop (1981) measured heat flow of 132 mW/m2 in a drill hole near Mount Meager, compared with a mean of 79 mW/m2 in three drill holes each more than 10 km from Mount Meager. Based on these studies, this volcano is one of the most promising geothermal targets in Canada and has been the subject of research since the 1970s (Jessop, 1998). However, three barriers to development have been identified and need to be addressed.

1. *Distance to the power grid.* This was a problem in the past, but it has improved in recent years as Innergex Renewable Energy Inc. has been operating two run-of-river hydroelectric plants since 2017. One is 5 km northeast of Mount Meager and the other is 7 km east of Mount Meager. Electricity generated at these two facilities is transmitted to the BC Hydro transmission system by a 230 kV transmission line (www.innergex.com/sites/boulder-creek). The proximity of this high-voltage line to Meager Creek has increased the economic feasibility of a potential geothermal power plant in the area.

2. *Landslide hazards.* A large rockslide and debris flow at Mount Meager on August 6, 2010 displaced millions of cubic metres of material (Allstadt, 2013; Guthrie et al., 2012). Meager Creek was temporarily dammed, and the flood risk led to the evacuation of 1500 Pemberton residents (Guthrie et al., 2012). Therefore, hazard assessment is an important consideration for ongoing geothermal development at Mount Meager.

3. *Uncertain permeability and porosity.* Geophysical studies that image the subsurface structure can help determine reservoir characteristics. This abstract is concerned with a 3-D resistivity model derived from inversion of magnetotelluric data. It is part of a multidisciplinary research program that includes magnetotellurics, passive seismic, gravity, bedrock mapping, fracture analysis, and thermal-spring geochemistry (Grasby et al., 2020).

Methods

The magnetotelluric (MT) method uses natural electromagnetic (EM) signals to image the electrical resistivity of the subsurface and is widely used in geothermal exploration (Muñoz, 2014). This EM method measures time series of electric and magnetic fields at the surface of the Earth, then converts them into frequency-domain transfer functions (TFs) that describe the impedance of the Earth. These TFs are used to calculate the electrical resistivity at depth. The MT method has two main advantages that make it suitable for geothermal exploration:

1. It can image aqueous and magmatic fluids, which are relevant to geothermal exploration. The resistivity of the crust varies over several orders of magnitude: dry crystalline rock has a resistivity more than 1000 Ωm, whereas the presence of aqueous fluids or partial melt can lower this to values in the range 1-10 Ωm. Thus, fluid-rich zones are readily distinguished in MT data.

2. It can resolve features over a broad range of depths, from the upper crust to the upper mantle, allowing for investigation of both fine-scale crustal structure and deeper resistivity anomalies. The frequency of the passive radio wave source controls the depth of exploration with high frequencies (e.g., kHz) giving information about shallow structures and low frequencies (e.g., μHz) giving information about deeper structures. This broad depth range is a distinct advantage over other EM methods that are more limited in scale.

The available MT data were recorded at 73 locations (Fig. 2a) and they included seven soundings collected in 1982 by the Pacific Geoscience Centre (Flores-Luna, 1986), 31 soundings collected in 2000 by Frontier Geosciences Inc. (Candy, 2001), and 35 soundings collected by the University of Alberta for this study. They included MT measurements at 23 sites in 2019 (Unsworth et al., 2020) and 12 sites in 2020. The time series were processed using statistically robust algorithms (Egbert & Eisel, 1998) based on the theory of Egbert and Booker (1986). The resistivity model was obtained from joint inversion of impedance and tipper data at 29 frequencies (0.001-400 Hz) and 66 sites (Fig. 2b). A 5% error floor was applied to the impedance data and a 0.03 absolute error floor was applied to the tipper data. The 3-D inversion algorithm ModEM developed by Kelbert et al. (2014) was used for the inversions.

The rectangular model mesh used in this study had 2.1 million cells: 148 in the north-south direction, 136 in the east-west direction, and 105 in the vertical direction. The cells were 250 x

250 m in the horizontal plane, with 15 padding cells increasing geometrically by a factor of 1.35 away from the central grid (Fig. 2b). The upper layers were 50 m thick, then layer thickness increased geometrically by a factor of 1.1 below topography. The top 12 layers, higher than all MT sites, were removed to decrease the total model size and the computing resources needed.

Multiple inversions were run to investigate sensitivity of the model to control parameters etc. and more inversions are in progress. The following steps are currently underway or in planning: (1) variation of smoothing parameters, e.g., regularization parameter (lambda) and covariance; (2) testing of different data subsets; and (3) testing of data sensitivity and model resolution, e.g., forward modelling and synthetic inversions. The initial half-space model had an r.m.s. misfit of ~12 and the inversions ended after 300-450 iterations with r.m.s. misfits of 2-4.

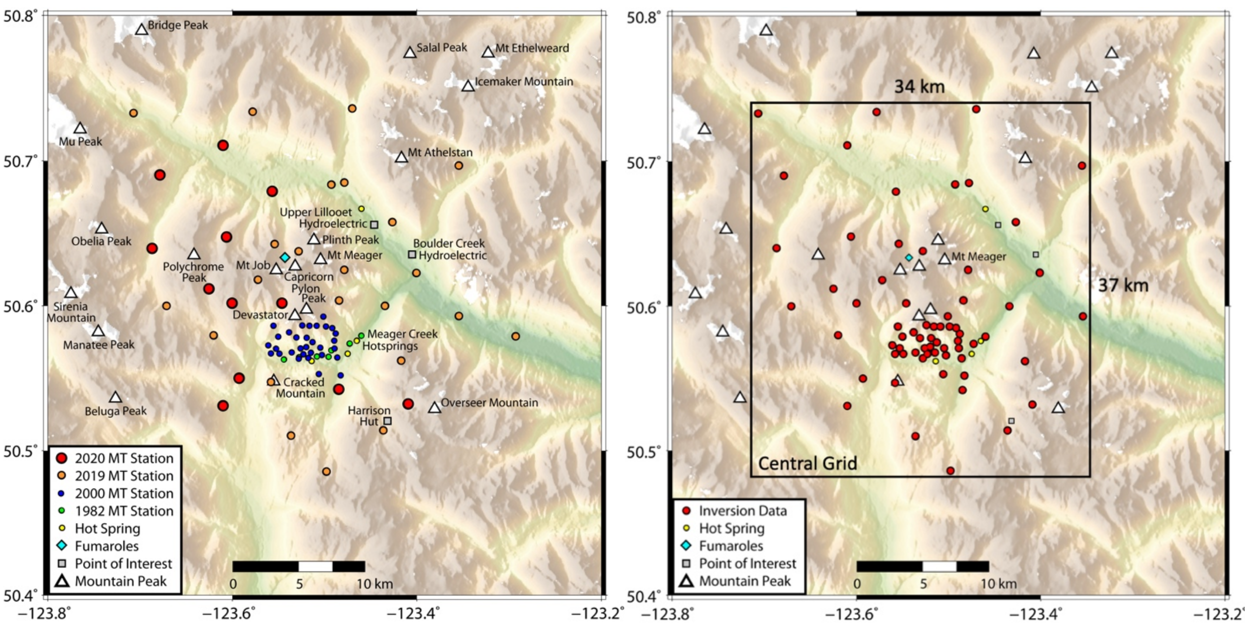

Figure 2*: (a) Map of the study area with all available MT data locations. (b) Locations used in the inversion.*

Results and Discussion

The inversion produced an inversion model that was found to be well resolved by the measured data. The uppermost kilometre of the Mount Meager massif is characterized by low resistivity, likely caused by saline aqueous fluids (brines) and hydrothermally altered rocks. There is a large conductor at 5-8 km below sea level, between Mount Meager and Meager Creek. It is > 7 km wide, > 10 km long and > 3 km thick. This anomaly is likely caused by brines and partially melted rocks, and it occurs beneath the areas investigated in 1982 and 2000 (Fig. 2a).

Ongoing analysis will include: (1) estimation of fluid content and relevant parameters using constraints from geophysical and geochemical experiments, (2) estimation of melt fraction using constraints from petrological experiments, and (3) joint interpretations using results from the gravity and seismic investigations.

Two general conclusions can be made: (1) there are near-surface brines and hydrothermally altered rocks beneath the Mount Meager massif, and (2) there is a magma body beneath the Mount Meager massif in the depth range 7-10 km. Detailed descriptions of these features will require further analysis; they will be provided at GeoConvention 2021, along with a finalized resistivity model. Implications for geothermal development are also being developed.

Acknowledgements

Funding was provided by an NSERC Discovery Grant to Martyn Unsworth and an award from the Future Energy Systems program at the University of Alberta. Additional resources and support were provided by NRCan and Geoscience BC. We thank G. Egbert, A. Kelbert and N. Meqbel for use of ModEM and Compute Canada for access to high-performance cluster computing. We thank S. Grasby, J. Craven, A. Williamson and Z. Vestrum for all of their help. Finally, we thank C. Candy at Frontier Geosciences for access to the 2000 MT data and the outstanding pilots from No Limits Helicopters.

References

Allstadt, K. (2013) Extracting source characteristics and dynamics of the August 2010 Mount Meager landslide from broadband seismograms: Seismic Inversion of Mount Meager Landslide. *Journal of Geophysical Research: Earth Surface*, **118(3)**, 1472–1490. https://doi.org/10.1002/jgrf.20110

Candy, C. (2001) Crew Development Corporation Report on a Magnetotelluric Survey, South Meager Geothermal Project, Pemberton, British Columbia (Project FGI-581; p. 168). Frontier Geosciences Inc.

Egbert, G. D., & Booker, J. R. (1986) Robust estimation of geomagnetic transfer functions. *Geophysical Journal International*, **87(1)**, 173–194. https://doi.org/10.1111/j.1365-246X.1986.tb04552.x

Egbert, G. D., & Eisel, M. (1998) EMTF: Programs for Robust Single Station and Remote Reference Analysis of Magnetotelluric Data: UNIX (and PC) Version.

Fairbank, B. D., Openshaw, R. E., Souther, J. G., & Stauder, J. J. (1981) Meager Creek Geothermal Project: An exploration case history. *Geothermal Resources Council Bulletin*, 1–7. https://doi.org/10.4095/103409

Flores-Luna, C. F. (1986) Electromagnetic induction studies over the Meager Creek geothermal area, British Columbia [PhD]. University of Toronto.

Grasby, S. E., Ansari, S. M., Calahorrano-Di Patre, A., Chen, Z., Craven, J. A., Dettmer, J., Gilbert, H., Hanneson, C., Harris, M., Liu, J., Muhammad, M., Russell, K., Salvage, R. O., Savard, G., Tschirhart, V., Unsworth, M. J., Vigouroux-Caillibot, N., & Williams-Jones, G. (2020) Geothermal resource potential of the Garibaldi volcanic belt, southwestern British Columbia (part of NTS 092J) (Report No. 2020–02; pp. 103–108). Geoscience BC.

Guthrie, R. H., Friele, P., Allstadt, K., Roberts, N., Evans, S. G., Delaney, K. B., Roche, D., Clague, J. J., & Jakob, M. (2012) The 6 August 2010 Mount Meager rock slide-debris flow, Coast Mountains, British Columbia: Characteristics, dynamics, and implications for hazard and risk assessment. *Natural Hazards and Earth System Sciences*, **12(5)**, 1277–1294. https://doi.org/10.5194/nhess-12-1277-2012

Hickson, C. J. (1994) Character of volcanism, volcanic hazards, and risk, northern end of the Cascade magmatic arc, British Columbia and Washington State. *Geological Survey of Canada Bulletin*, **481**, 231–250. https://doi.org/10.4095/203253

Jessop, A. M. (1998) Geothermal Energy in Canada. *Geoscience Canada*, **25(1)**, 33–41.

Jones, A. (2019) Geothermal Abundance in the Cascade Range (Washington / Oregon / N. California). *IOP Conf. Ser.: Earth Environ. Sci.*, **249**, 012012, IOP Publishing. doi:10.1088/1755-1315/249/1/012012

Kelbert, A., Meqbel, N., Egbert, G. D., & Tandon, K. (2014) ModEM: A modular system for inversion of electromagnetic geophysical data. *Computers & Geosciences*, **66**, 40–53. https://doi.org/10.1016/j.cageo.2014.01.010

Lewis, J. F., & Jessop, A. M. (1981) Heat flow in the Garibaldi volcanic belt, a possible Canadian geothermal energy resource area. *Canadian Journal of Earth Sciences*, **18**, 366–375. https://doi.org/10.1139/e81-028

Mullen, E. K., Weis, D., Marsh, N. B., & Martindale, M. (2017) Primitive arc magma diversity: New geochemical insights in the Cascade Arc. *Chemical Geology*, **448**, 43–70. https://doi.org/10.1016/j.chemgeo.2016.11.006

Muñoz, G. (2014) Exploring for Geothermal Resources with Electromagnetic Methods. *Surveys in Geophysics*, **35(1)**, 101–122. https://doi.org/10.1007/s10712-013-9236-0

Savard, G., Bostock, M.G. & Christensen, N.I. (2018) Seismicity, Metamorphism, and Fluid Evolution Across the Northern Cascadia Fore Arc. *Geochemistry, Geophysics, Geosystems*, **19**, 1881–1897. https://doi.org/10.1029/2017GC007417

Souther, J. G. (1981) Canadian Geothermal Research Program. *American Association of Petroleum Geologists*, **177**, 391–400.

Stern, R. J. (2002) Subduction zones. *Reviews of Geophysics*, **40(4)**, 1012. https://doi.org/10.1029/2001RG000108

Unsworth, M. J., Hanneson, C., & Williamson, A. R. (2020) Broadband magnetotelluric study at Mount Meager to investigate the hydrothermal and magmatic system (Report No. 2020–09; Chapter 5, pp. 77–100). Geoscience BC.